ISSN 0016-7037
Volume 74, Number 17
September 1, 2010

ELSEVIER

Geochimica et Cosmochimica Acta

JOURNAL OF THE GEOCHEMICAL SOCIETY
AND THE METEORITICAL SOCIETY

Volume 74, Number 17 September 1, 2010

Articles

Continued on outside back cover

Available online at www.sciencedirect.com
ScienceDirect
Geochimica et Cosmochimica Acta 74 (2010) 4988–5001
Geochimica et Cosmochimica Acta
www.elsevier.com/locate/gca

Physiological and isotopic responses of scleractinian corals to ocean acidification

Shani Krief [a,b], Erica J. Hendy [c,*], Maoz Fine [a,b], Ruth Yam [d], Anders Meibom [e], Gavin L. Foster [c], Aldo Shemesh [d]

[a] The Interuniversity Institute for Marine Science in Eilat, P.O. Box 469, Eilat 88103, Israel
[b] The Mina & Everard Goodman Faculty for Life Sciences, Bar-Ilan University, Ramat Gan 52900, Israel
[c] Department of Earth Sciences, University of Bristol, Bristol, UK
[d] Department of Environmental Sciences and Energy Research, The Weizmann Institute of Science, Rehovot 76100, Israel
[e] Laboratoire de Mineralogie et Cosmochimie du Museum (LMCM), Museum National d'Histoire Naturelle, Paris, France

Received 1 February 2010; accepted in revised form 17 May 2010; available online 1 June 2010

Abstract

Uptake of anthropogenic CO_2 by the oceans is altering seawater chemistry with potentially serious consequences for coral reef ecosystems due to the reduction of seawater pH and aragonite saturation state (Ω_{arag}). The objectives of this long-term study were to investigate the viability of two ecologically important reef-building coral species, massive *Porites* sp. and *Stylophora pistillata*, exposed to high pCO_2 (or low pH) conditions and to observe possible changes in physiologically related parameters as well as skeletal isotopic composition. Fragments of *Porites* sp. and *S. pistillata* were kept for 6–14 months under controlled aquarium conditions characterized by normal and elevated pCO_2 conditions, corresponding to pH_T values of 8.09, 7.49, and 7.19, respectively. In contrast with shorter, and therefore more transient experiments, the long experimental timescale achieved in this study ensures complete equilibration and steady state with the experimental environment and guarantees that the data provide insights into viable and stably growing corals. During the experiments, all coral fragments survived and added new skeleton, even at seawater $\Omega_{arag} < 1$, implying that the coral skeleton is formed by mechanisms under strong biological control. Measurements of boron (B), carbon (C), and oxygen (O) isotopic composition of skeleton, C isotopic composition of coral tissue and symbiont zooxanthellae, along with physiological data (such as skeletal growth, tissue biomass, zooxanthellae cell density, and chlorophyll concentration) allow for a direct comparison with corals living under normal conditions and sampled simultaneously. Skeletal growth and zooxanthellae density were found to decrease, whereas coral tissue biomass (measured as protein concentration) and zooxanthellae chlorophyll concentrations increased under high pCO_2 (low pH) conditions. Both species showed similar trends of $\delta^{11}B$ depletion and $\delta^{18}O$ enrichment under reduced pH, whereas the $\delta^{13}C$ results imply species-specific metabolic response to high pCO_2 conditions. The skeletal $\delta^{11}B$ values plot above seawater $\delta^{11}B$ vs. pH borate fractionation curves calculated using either the theoretically derived α_B value of 1.0194 (Kakihana et al. (1977) *Bull. Chem. Soc. Jpn.* **50**, 158) or the empirical α_B value of 1.0272 (Klochko et al. (2006) *EPSL* **248**, 261). However, the effective α_B must be greater than 1.0200 in order to yield calculated coral skeletal $\delta^{11}B$ values for pH conditions where $\Omega_{arag} \geqslant 1$. The $\delta^{11}B$ vs. pH offset from the seawater $\delta^{11}B$ vs. pH fractionation curves suggests a change in the ratio of skeletal material laid down during dark and light calcification and/or an internal pH regulation, presumably controlled by ion-transport enzymes. Finally, seawater pH significantly influences skeletal $\delta^{13}C$ and $\delta^{18}O$. This must be taken into consideration when reconstructing paleo-environmental conditions from coral skeletons.

* Corresponding author. Address: Department of Earth Sciences, University of Bristol, Wills Memorial Building, Queens Rd., Bristol BS6 5UQ, UK. Tel.: +44 117 331 5003.
E-mail address: e.hendy@bristol.ac.uk (E.J. Hendy).

0016-7037/$ - see front matter © 2010 Elsevier Ltd. All rights reserved.
doi:10.1016/j.gca.2010.05.023

1. INTRODUCTION

Atmospheric CO_2 concentration has increased from pre-industrial levels of 280 ppmv to over 380 ppmv, the highest concentration over the last 800,000 years (Luthi et al., 2008). By the end of this century, atmospheric CO_2 concentration is predicted to double relative to pre-industrial levels as a direct result of human activity (Solomon et al., 2007). Approximately a quarter of anthropogenic CO_2 is being absorbed by the ocean (Sabine et al., 2004; Canadell et al., 2007), and at the current rate of CO_2 uptake the average surface ocean pH will drop from 8.2 to 7.8 by the end of 2100 (Caldeira and Wickett, 2005). This represents a shift in seawater pH to levels below those experienced by marine organisms during the last several million years (Pearson and Palmer, 2000). The associated decrease in seawater carbonate ion concentration [CO_3^{2-}] could substantially impact calcifying organisms, such as scleractinian corals, by lowering the saturation of ocean water with respect to the carbonate mineralogy of their skeletons (Gattuso et al., 1998; Kleypas et al., 1999a; Leclercq et al., 2000; Orr et al., 2005; Schneider and Erez, 2006; Anthony et al., 2008; Marubini et al., 2008). The aragonite saturation state (Ω_{arag}) is defined as:

$$\Omega_{arag} = \frac{[Ca^{2+}] \cdot [CO_3^{2-}]}{K'_{arag}} \quad (1)$$

where K'_{arag} is the apparent solubility product of the mineral. Values of $\Omega_{arag} > 1$ indicate supersaturation, whereas $\Omega_{arag} < 1$ is undersaturated. Coral reefs in the modern ocean are restricted to regions where seawater Ω_{arag} exceeds 3.3 (Kleypas et al., 1999b). Modeling of future Ω_{arag} indicates that by 2040 surface waters in regions like the Australian Great Barrier Reef will become marginal for coral calcification (Kleypas et al., 2006) potentially threatening the existence of these unique ecosystems.

Accurate predictions of the viability of coral reef ecosystems under conditions of ocean acidification require information on how coral physiology and calcification will respond (Kleypas et al., 2006). In particular, the effect of ocean acidification on the relationship between the symbiotic photosynthetic algae (zooxanthellae) contained within the tissue of most coral and the calcification of the coral's aragonite skeleton. Zooxanthellae activity strongly stimulates calcification; during daylight, when the algae are photosynthesizing, calcification rates are 3–4 times greater than in the dark (Gattuso et al., 1999; Furla et al., 2000). However, the explanation for how zooxanthellae photosynthesis and coral calcification are connected remains controversial (Muscatine, 1990; Gattuso et al., 1999; Cohen and McConnaughey, 2003; Schneider and Erez, 2006).

In this study, we have investigated the response of scleractinian reef-forming corals and their zooxanthellae after long-term (up to 14 months) exposure to normal and reduced pH conditions (8.09, 7.49, and 7.19 on the pH_T scale). Corals in the low-end pH treatment were exposed to extremely high pCO_2 (equivalent to seven times the predicted CO_2 level by 2100), to investigate the physiological response at $\Omega_{arag} < 1$ and its translation into skeletal C, O, and B isotopic signatures. Two zooxanthellate coral species with very different life strategies were studied to provide information on the range of potential responses. The massive *Porites* sp. form large multi-century old colonies and calcify relatively slowly (extending 1–2 cm yr^{-1}), whereas the branching *Stylophora pistillata* is short-lived and deposits skeleton rapidly. The responses of both species to shifts in CO_2 and seawater carbonate chemistry were monitored using isotopic tracers (skeletal $\delta^{11}B$, $\delta^{13}C$, and $\delta^{18}O$, and coral tissue and zooxanthellae $\delta^{13}C$) and key physiological parameters including skeletal growth, tissue biomass, zooxanthellae cell density, and chlorophyll concentration.

The isotopic systems ($\delta^{11}B$, $\delta^{18}O$, and $\delta^{13}C$) investigated in this study are often used as palaeo-environmental proxies. Skeletal $\delta^{18}O$ is the most commonly used proxy for seawater temperature and salinity (Cole et al., 2000; Gagan et al., 2000; Hendy et al., 2002; Al-Rousan et al., 2003; Asami et al., 2004; Linsley et al., 2006). Skeletal, tissue, and zooxanthellae $\delta^{13}C$ has been used to trace seawater carbonate chemistry and metabolic processes that cause preferential addition or subtraction of ^{12}C from the internal DIC pool through respiration and photosynthesis (Risk et al., 1994; McConnaughey et al., 1997; Grottoli, 1999, 2002; Grottoli and Wellington, 1999; Heikoop et al., 2000; Asami et al., 2004; Swart et al., 2005; Omata et al., 2008). 'Vital effects' during the biomineralization of the coral skeleton have been observed to shift both $\delta^{13}C$ and $\delta^{18}O$ values (McConnaughey, 1989b; Allison et al., 1996; Heikoop et al., 2000; Omata et al., 2008). Since many potential sources of 'vital effects' are pH sensitive physiological processes (e.g., zooxanthellae photosynthetic activity, polyp metabolism, calcification rate), ocean acidification may also affect these skeletal isotopic tracers. Investigations into the effect of seawater pH on coral $\delta^{18}O$ and $\delta^{13}C$ are limited and there are no studies of species-specific variation of $\delta^{18}O$ and $\delta^{13}C$ in a controlled pCO_2 system.

Reconstruction of past seawater pH levels may assist in understanding future impacts of reduced oceanic pH on corals and their resilience to ocean acidification. The boron isotopic composition ($\delta^{11}B$) of marine carbonates is used as a proxy for reconstructing paleo-pH, as applied in studies of experimentally cultured (Hönisch et al., 2004; Reynaud et al., 2004) and retrieved corals (Hemming and Hanson 1992; Hemming et al., 1998; Pelejero et al., 2005; Kasemann et al., 2009; Wei et al., 2009). The relative concentration of boric acid [$B(OH)_3$] and the borate ion [$B(OH)_4^-$], the two main boron species in the ocean, is pH dependent and there is a ~27‰ difference in $\delta^{11}B$ between these two species (Klochko et al., 2006). Environmental variables such as water temperature, irradiance, food supply, and water depth have been shown to have little effect on bulk $\delta^{11}B$ values of coral skeleton (Hönisch et al., 2004; Reynaud et al., 2004). However, 'vital effects' have been implicated in micron-scale skeletal $\delta^{11}B$ variations measured in both deep-sea (i.e., non-zooxanthellate) and shallow-water (i.e., zooxanthellate) corals by Secondary Ion Mass Spectrometry (SIMS) (Rollion-Bard et al., 2003; Blamart et al., 2007). As a result, fundamental questions remain regarding the degree to which bulk B isotopic compositions of

shallow-water scleractinian corals correlate with changes in water pH and the degree to which species-dependent 'vital effects' perturb this relationship (Hönisch et al., 2004; Blamart et al., 2007).

2. MATERIALS AND METHODS

2.1. Experimental design

Two colonies of *Porites* sp. and four colonies of *S. pistillata* were collected in July 2007 from the reef in front of the Interuniversity Institute for Marine Science in Eilat, Israel (IUI) (29°30′N, 34°55′E), at 8 m depth. Following fragmentation, pieces were glued to pre-labeled glass slides. After a one-month recovery period the fragments were dyed with Alizerine Red (Sigma–Aldrich, USA) in order to mark the beginning of the experiment in the skeleton, and 20 fragments of each species were transferred to each of the three pH_T treatments: 8.09 ($pCO_2 = 387$ μatm; ambient), 7.49 ($pCO_2 = 1908$ - *μatm),* and 7.19 ($pCO_2 = 3976$ μatm) (Table 1). Corals were maintained in a water table with a seawater flow-through system. Seawater was pumped from a depth of 30 m into 1000 L tanks where the pH was regulated. A pH electrode (S-200C, Sensorex, CA, USA) was located in each tank and connected to a pH controller (Aquastar, IKS ComputerSysteme GmbH, Karlsbad, Germany), which monitored the pH and bubbled CO_2 (from a CO_2 cylinder) to each tank according to the desired pH. Daily pH variability was low (±0.05) throughout the experiment and no major fluctuations were recorded. Well-mixed filtered (500 μm) water from each tank continuously flowed into the corresponding section (150 L) of the water table. All pH data were recorded using monitoring software (Timo, Matuta, Germany) on the NBS scale. The pH_{NBS} data were shifted onto the total pH_T scale by subtracting −0.11, which includes a minor correction for $[SO_4^{2-}]$ and the stability constant of HSO_4^- at a salinity of 40.7.

Temperature was regulated to ~25 °C using a combination of an array of 300 W BluClima aquarium heaters (Ferplast Spa, Vicenza, Italy) and a water cooler (custom-made at IUI). Light (200 ± 20 μmol m^{-2} s^{-1}, 10L:14D photoperiod) was provided by three metal halide lamps (400 W/D, Osram GmBH, Germany). Data were recorded hourly using HOBO Pendant Temp/Light Data Loggers (Pocasset, MA, USA).

After an incubation period (6 months for *S. pistillata* and 7 months for *Porites* sp.) a set of fragments was sampled (nine fragments of *S. pistillata* and five fragments of *Porites* sp. from each treatment), processed, and analyzed for isotopic composition of coral tissue ($\delta^{13}C$), zooxanthellae ($\delta^{13}C$) and the coral skeleton ($\delta^{13}C$, $\delta^{18}O$, $\delta^{11}B$). Fourteen months from the beginning of the experiment, an additional five fragments of each species from each treatment were taken for zooxanthellae cell density, chlorophyll *a* concentration, and host protein concentration measurements. Water samples from the treatment basins were collected throughout the experiment to monitor $\delta^{18}O$ of H_2O and $\delta^{13}C$ of dissolved inorganic carbon (DIC).

Two multiple comparison methods were used to statistically examine the results; least significant difference (LSD) and the Tukey test. The LSD is a less restrictive test and was used to indicate some trends found in the physiological results that were not identified using the Tukey test.

Table 1
Carbonate chemistry and isotopic composition of seawater in the three pH treatments. DIC, Ω_{arag}, and pCO_2 values were calculated from the pH and alkalinity measurements using the program CO2SYS.XLS (Lewis and Wallace, 1998; Pierrot et al., 2006) selecting K_1 and K_2 carbonic acid dissociation constants of Mehrbach et al. (1973), as refit by Dickson and Millero (1987), and K_{SO_4} as determined by Dickson (1990).

pH total scale	DIC (μmol kg^{-1})	Ω_{arag}	Alkalinity (μmol kg^{-1})	pCO_2 (μatm)	$\delta^{13}C$ (‰)	$\delta^{18}O$ (‰)
8.09	2108	3.99	2485	385	0.87	1.92
7.49	2412	1.25	2479	1904	−4.03	2.00
7.19	2532	0.65	2485	3970	−5.81	1.97

2.2. Separation of coral tissue and zooxanthellae

Coral tissue was removed using an airbrush containing filtered sea water (FSW); the sea water was filtered with a 0.2 μm filter using a vacuum pump (Rocker 300, Rocker Scientific Co., Ltd., Taiwan). The filtered seawater containing the tissue extract was homogenized with an electric homogenizer (DIAX 100 homogenizer Heidolph Instruments GmbH & Co., KG, Schwabach, Germany) for 10 s and centrifuged for 10 min at 5000 rpm (rcf 2500 m/s^2; centrifuge 4K15 Sigma laborzentrifugen GmbH, Osterode, Germany). The supernatant (containing coral tissue) was separated from the pellet (zooxanthellae) and centrifuged for 5 min at 5000 rpm (rcf 2500 m/s^2) to remove remaining zooxanthellae. The supernatant was inspected under a microscope (D-Eclipse, Nikon, Japan) to confirm removal of all zooxanthellae and was centrifuged again if necessary, and then filtered through a GF/F filter (Whatman) using a vacuum pump. Filters, containing coral tissue, were washed with double-distilled water (DDW) to remove salts and dried overnight at 50 °C in a glass vial. The pellet, containing the zooxanthellae, was resuspended in FSW, homogenized, and centrifuged. It was then treated with 1 ml HCl (5%) to remove $CaCO_3$. This treatment has been proven to have no influence on the isotopic composition (Heikoop et al., 1998). Following centrifugation and removal of the acid, the sample was washed with FSW several times. In order to remove salts the pellet was washed with DDW and then dried overnight at 50 °C.

Separation of coral tissue and zooxanthellae for cell density, chlorophyll concentration, and protein concentration were done in a similar manner. After first centrifugation, the total volume was measured and 200 μl of the supernatant was removed for host protein analysis. The pellet was resuspended with FSW, homogenized, and centrifuged for 5 min at 5000 rpm (rcf 2500 m/s^2). The procedure was repeated two more times in order to remove remaining tissue. Zooxanthellae were then resuspended in 1 ml FSW for cell count. The cell numbers were estimated by photography using a digital camera (CoolPix 995, Nikon, Japan) attached to a microscope (YS100, Nikon, Japan). Each image represents a total volume of 0.1 μl. Cells were counted manually on the computer screen and multiplied by 10,000 in order to get total cells present in each sample. Chlorophyll *a* was extracted in 1 ml acetone (95%) at 4 °C for 10 h. Concentrations were calculated using spectrophotometry (Ultrospec 2100 pro, GE Bioscience, USA) and the standard equations (Jeffrey and Humphrey, 1975). Coral surface area was measured using the paraffin-wax method of Stimson and Kinzie (1991).

Host protein concentrations were analyzed using the Quick Start Bradford Protein Assay Kit (Bio-Rad Laboratories, Hercules, CA, USA). Optical density was read at 595 nm using an ELISA reader (PowerWave XS, BioTek, USA). Concentrations were calculated based on Quick Start Bovine Serum Albumin Standard Set (Bio-Rad Laboratories, Hercules, CA, USA). Results were multiplied by total volume in order to get the total amount of protein (μg). Total protein to surface area ratio was calculated representing changes in coral biomass.

2.3. Skeletal growth measurements

Skeletal growth was measured based on changes in skeletal surface area on the slide and changes in buoyant weight (only for *S. pistillata*). For surface area measurements, photos taken by digital camera (CoolPix 8400, Nikon, Japan) were analyzed using image analysis software (ImageJ, V. 1.37 m, National Institute of Health, USA). Coral weight was measured at the beginning and the end of the experiment by buoyant weighing (Davies, 1989) using a Vibra balance (Shinko Denshi Co., Ltd., Japan) (accuracy ~1 mg). Relative skeletal growth was calculated based on the net growth divided by the original surface area or weight.

2.4. Skeleton sampling

To remove remaining organic matter, skeleton fragments were soaked in 30% hydrogen peroxide, sonicated for 4 min at 20 °C, and incubated overnight at room temperature. This treatment is proven to have no influence on the isotopic composition (of C and O; Boiseau and Juillet-Leclerc, 1997). Skeletons were then washed several times with DDW and were dried overnight at 50 °C. Newly-grown material was collected from the glass slide, using a scalpel, and ground into a powder.

2.5. Carbon and oxygen isotopic composition

For skeletal $\delta^{13}C$ and $\delta^{18}O$ analysis, 220–250 μg of powdered skeleton was acidified in dried concentrated phosphoric acid (H_3PO_4). Head space CO_2 gas was analyzed using a Finnigan MAT 252 mass spectrometer connected online to a GasBench II. $\delta^{13}C$ and $\delta^{18}O$ data are reported in permil units (‰) relative to V-PDB (Vienna-PeeDee Belemnite Limestone) standard. Measurements were monitored using a laboratory working standard introduced in-between samples. The long-term precision of replicated analysis of our internal laboratory standard is 0.06‰ and 0.10‰ (2σ) for carbon and oxygen, respectively.

Measurements of $\delta^{13}C$ of DIC were performed on samples that were collected from the water table throughout the experiment, according to the coral skeleton protocol using 1 ml water sample. When collected, samples were poisoned using 1 ml saturated $HgCl_2$ solution in 60 ml water to prevent any further biological activity that might change their isotopic composition.

The $\delta^{13}C$ composition in coral tissue and zooxanthellae was measured using an elemental analyzer-isotopic ratio mass spectrometer (EA-IRMS) standard protocol, using 220–250 μg organic matter for each sample. The sample was "flash combusted" to convert all organic substances into combustion products by instantaneous and complete oxidation, followed by reduction reactions. Calibrated working standards were introduced in-between samples and compared to the Vienna International Atomic Energy Agency standards. Precision of measurements for $\delta^{13}C$ was 0.05‰ (2σ). The $\delta^{13}C$ values are reported in permil units relative to the Vienna-PeeDee Belemnite international standard.

Seawater $\delta^{18}O$ measurements are based on the classical procedure of equilibration of water with carbon dioxide (Epstein and Mayeda, 1953) modified to Continuous Flow Isotope Ratio Mass Spectrometry (Nelson, 2000). A 0.5 ml water sample was slightly acidified using phosphoric acid. Vials were flushed with a mixture of 0.5% carbon dioxide in helium, after reaching full equilibration with the seawater headspace. The CO_2 gas was analyzed for $\delta^{18}O$ using a Finnigan MAT 252 mass spectrometer connected online to a GasBench II. Data are reported in permil units relative to V-SMOW. Internal working standards were introduced in-between samples. The precision of replicated analysis is better than 0.1‰ (2σ).

2.6. Boron isotopic composition

For B isotope analyses, 3 mg of skeletal material was screened under a microscope to exclude any remaining tissue or extraneous material. The skeleton was powdered, then cleaned, and dissolved following the standard procedure, with the exception of the clay removal step, described in Barker et al. (2003) for foraminiferal trace element analysis. The samples were dissolved in 0.5 HNO_3 and buffered (pH ~ 5) by the addition of Na acetate/acetic acid prior to being passed through an anion exchange resin (63–120 μm B-specific Amberlite RA 743 resin) to separate B. The carbonate matrix was eluted with repeated rinses of MQ before the separated B was collected with 0.5 M HNO_3. Total procedural blanks typically ranged from 70 to 100 pg and the column yield for this procedure is ~95% and results in no significant isotopic fractionation (Foster, 2008). Measurements were made on a Thermo-Finnigan Neptune MC-ICP-MS (University of Bristol) following the method outlined in Foster (2008). A PFA spray chamber with a ~3 mL/min add gas of NH_3, ported in immediately after sample introduction through a PFA 50 μL/min nebuliser, maintains basic conditions within the spray chamber and a fast wash-out time. Solution concentrations were 50–100 ng mL^{-1} B. Boron isotopes were determined by 2 min simultaneous collection of $^{11}B^+$ and $^{10}B^+$ using Faraday cups. Each sample was analyzed a minimum of two times and the mean value used. Instrumental mass bias was corrected using the mean of bracketing, intensity-matched NIST SRM 951 boric acid reference material. Results are presented relative to NIST SRM 951 in the conventional δ-notation ($\delta^{11}B$). The uncertainty based on repeat measurements ($n = 18$) of a fully processed in-house coral reference material is ±0.25‰ (2σ).

3. RESULTS

All corals survived throughout the 14 months of the experiment and new skeletal growth was observed on the glass slides under all three experimental conditions. We also note that corals from the same batch, which were not harvested, are still alive and continue to add skeletal material at the time this paper was written, 28 months after the beginning of the experiment.

3.1. Cell density, chlorophyll *a*, and host protein

Coral biomass, as measured by the mass of host protein per surface area, varied between pH treatments in both species (Fig. 1A). Biomass of *Porites* sp. was 0.17% lower at pH_T 8.09 as compared to pH_T 7.49 and 7.19 (one-way ANOVA, LSD, $p < 0.05$). Biomass of *S. pistillata* at pH_T 8.09 was 0.42% and 0.5% lower as compared to pH_T 7.49 and 7.19, respectively (one-way ANOVA, Tukey, $p < 0.05$).

Both species showed similar variations in zooxanthellae cell density between pH treatments. Zooxanthellae cell per surface area (Fig. 1B) and per mg protein (Fig. 1C) in *Porites* sp. was significantly higher (one-way ANOVA, Tukey, $p < 0.05$) at pH_T 8.09 than at pH_T 7.49 and 7.19. In *S. pistillata*, zooxanthellae cell density was significantly higher at pH_T 8.09 than at pH_T 7.49 (one-way ANOVA, Tukey, $p < 0.05$).

Chlorophyll concentration per cell (Fig. 1D) was significantly higher at pH_T 7.19 as compared to pH_T 8.09 and 7.49 in both species (one-way ANOVA, Tukey, $p < 0.05$). In *Porites* sp. chlorophyll concentration per cell was 31%

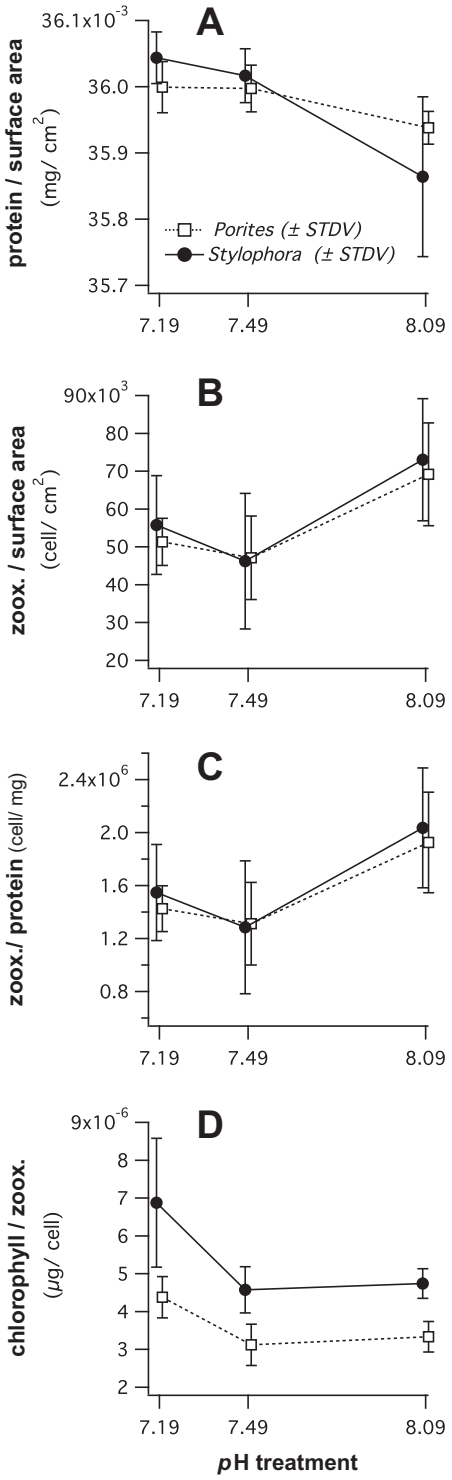

Fig. 1. Physiological responses of *S. pistillata* and *Porites* sp. cultured at normal (8.09) and reduced (7.49 and 7.19) pH conditions (mean ± SD). (A) Coral biomass (protein content relative to surface area in mg/cm^2); $n = 5$ for each treatment. (B) zooxanthellae cell density relative to surface area (cells/cm^2); $n = 4$–5 for each treatment. (C) Zooxanthellae cell density relative to protein content (cells/mg); $n = 4$–5 for each treatment. (D) chlorophyll content per zooxanthellae (µg/cell); $n = 4$–5 for each treatment.

lower at pH_T 8.09 than at pH_T 7.19 whereas in *S. pistillata* it was only 23% lower.

3.2. Skeletal growth

Calcification in both species was significantly slower under decreased pH (Fig. 2) (one-way ANOVA, Tukey, $p < 0.05$). *Porites* sp. showed a 55% and 75% drop in growth (some fragments exceeded twofold their original size, thus values surpass 100%) of skeletal surface area between pH_T 8.09 and pH 7.49 and 7.19, respectively. *S. pistillata* showed a ~60% drop in skeletal growth of skeletal surface area between pH_T 8.09 and the lower pH treatments (7.49 and 7.19). Skeletal growth for *S. pistillata* estimated by buoyant weight showed an 18% decrease between pH_T 8.09 and pH_T 7.49 and 7.19 (Fig. 2B). No significant differences were found between skeletal growth at pH_T 7.49 and 7.19 in both species. This variation in relative skeletal growth decrease obtained by different methods suggests that skeletal morphological changes also occurred.

3.3. Isotopic composition of DIC and seawater

The $\delta^{13}C$ values of DIC varied between treatments (one-way ANOVA, Tukey, $p < 0.05$; Table 1) because CO_2 from the cylinder had lower $\delta^{13}C$ values than atmospheric CO_2, resulting in lighter $\delta^{13}C$ at higher pCO_2 (reduced pH). Vari-

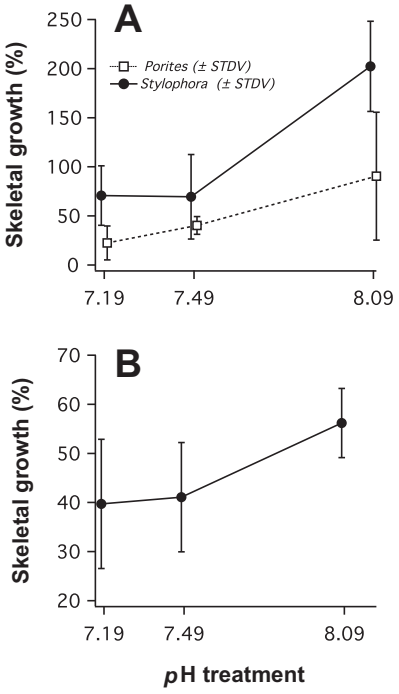

Fig. 2. Percent skeletal growth of *S. pistillata* (after three months) and *Porites* sp. (after thirteen months) cultured at normal (8.09) and reduced (7.49 and 7.19) pH conditions (mean ± SD); $n = 7$–12 for each treatment. (A) Skeletal growth measured by changes in surface area on the slides. (B) Skeletal growth measured by buoyant weighing of *S. pistillata*.

ations of up to 4‰ in $\delta^{13}C$ between cylinders were recorded (cylinders were replaced approximately once per month). The $\delta^{13}C$ of DIC averaged between 0.87‰, −4.03‰, and −5.81‰ for pH_T 8.09, 7.49, and 7.19, respectively. The $\delta^{13}C$ of the resulting coral skeleton and tissue has to be corrected for this reservoir effect in order to be able to compare it with $\delta^{13}C$ obtained under natural pCO_2 conditions. Therefore, in high pCO_2 experiments, the $\delta^{13}C$ of the coral skeleton and tissue are reported as the deviation in permil relative to the average isotopic composition of the DIC in each tank. These reservoir-corrected carbon isotopic compositions are referred to as $\Delta^{13}C$. Seawater $\delta^{18}O$ values showed no specific trend between pH treatments and insignificant variations over time.

3.4. Isotopic composition of zooxanthellae and coral tissue

Both coral species recorded a drop in tissue and zooxanthellae $\Delta^{13}C$ values under reduced pH (Fig. 3A, B and Table 2). *S. pistillata* tissue and zooxanthellae $\Delta^{13}C$ values were 5.5‰ and 7‰ lighter in pH_T 7.49 and 7.19, respectively, than at pH_T 8.09 (one-way ANOVA, Tukey, $p < 0.05$). In *Porites* sp. tissue $\Delta^{13}C$ was 1.6‰ and 1‰ lighter in pH_T 7.49 and 7.19, respectively, than at pH_T 8.09 (one-way ANOVA, Tukey, $p < 0.05$). Zooxanthellae $\Delta^{13}C$ in *Porites* sp. showed larger variations: it was 2.7‰ and 3.5‰ lighter at pH_T 7.49 and 7.19, respectively, than at pH_T 8.09 (one-way ANOVA, Tukey, $p < 0.05$).

3.5. Isotopic composition of coral skeleton

Stylophora pistillata skeletal $\Delta^{13}C$ showed no significant difference between treatments (Fig. 3C and Table 2). In *Porites* sp. skeletal $\Delta^{13}C$ values were depleted by 2.3‰ and 1.5‰ between pH_T 8.09 and 7.49 and between pH_T 8.09 and 7.19, respectively (one-way ANOVA, Tukey, $p < 0.05$). Skeletal $\delta^{18}O$ values were enriched in both species under reduced pH (Fig. 3D and Table 2) (one-way ANOVA, Tukey, $p < 0.05$). In *S. pistillata* $\delta^{18}O$ was 0.3‰ heavier at pH_T 7.49 and 7.19 than at pH_T 8.09. In *Porites* sp. $\delta^{18}O$ was 0.5‰ and 0.7‰ heavier at pH_T 7.49 and 7.19, respectively, than at pH_T 8.09.

Boron isotopic composition in both species showed a clear dependence on pH (Fig. 4 and Table 2) (one-way ANOVA, Tukey, $p < 0.05$). To compare the measured coral $\delta^{11}B$ with expected values according to pH dependent isotopic fractionation of borate, boron–pH curves were plotted (Fig. 4) using the following equation:

$$\mathrm{pH} = \mathrm{p}K_B^* - \log\left[-\frac{\delta^{11}B_{sw} - \delta^{11}B_{coral}}{\delta^{11}B_{sw} - \alpha_B\delta^{11}B_{coral} - (\alpha_B - 1) * 10^3}\right] \quad (2)$$

where the equilibrium constant pK_B^* is 8.5682 for the experimental temperature of 25 °C and a salinity of 40.7, the isotopic composition of seawater ($\delta^{11}B_{sw}$) is 39.5‰, and α_B is the fractionation factor ($^{11,10}K_B$) between $B(OH)_4^-$ and $B(OH)_3$ at 25 °C. We discuss our B isotope data using two different α_B values; the derived and widely used value

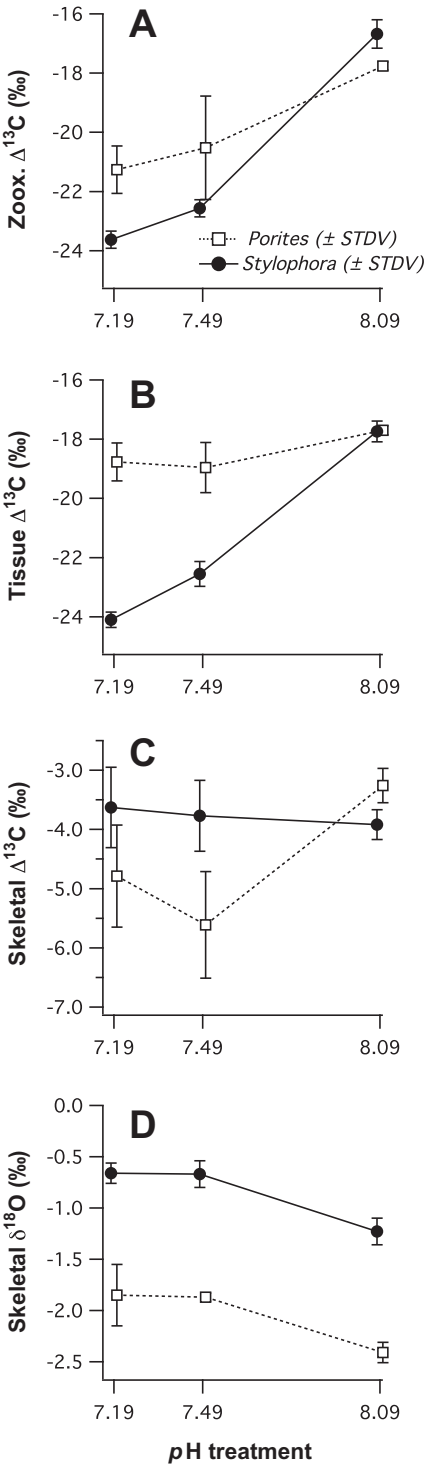

Fig. 3. Isotopic response of *S. pistillata* and *Porites* sp. cultured at normal (8.09) and reduced (7.49 and 7.19) pH conditions. All $\delta^{13}C$ values are reported as $\Delta^{13}C$, the deviation in permil relative to the average $\delta^{13}C$ composition of the sea water DIC in each treatment (mean ± SD). (A) $\delta^{13}C$ in zooxanthellae $n = 4$–5 in *Porites* sp. and $n = 5$–8 for *S. pistillata*. (B) $\delta^{13}C$ in tissue; $n = 4$–5 in *Porites* sp. and $n = 5$–8 for *S. pistillata*. (C) $\delta^{13}C$ in skeleton; $n = 4$–5 in *Porites* sp. and $n = 5$–8 for *S. pistillata*. (D) $\delta^{18}O$ in skeleton; $n = 4$–5 in *Porites* sp. and $n = 4$–8 for *S. pistillata*. (mean ± SD).

Table 2
Isotopic composition of coral skeleton, tissue, and zooxanthellae in the studied species (mean in ‰ ± SD).

pH treatment	$\Delta^{13}C$ skeleton	$\Delta^{13}C$ tissue	$\Delta^{13}C$ zooxanthellae	$\delta^{18}O$	$\delta^{11}B$
Porites sp.					
8.09	−3.26 ± 0.29	−17.70 ± 0.15	−17.76 ± 0.14	−2.41 ± 0.10	25.24 ± 0.20
7.49	−5.61 ± 0.90	−18.96 ± 0.85	−20.52 ± 1.75	−1.87 ± 0.04	21.95 ± 0.04
7.19	−4.79 ± 0.86	−18.77 ± 0.64	−21.26 ± 0.80	−1.85 ± 0.30	20.97 ± 0.40
S. pistillata					
8.09	−3.92 ± 0.25	−17.74 ± 0.35	−16.68 ± 0.48	−1.23 ± 0.13	24.76 ± 0.13
7.49	−3.77 ± 0.60	−22.55 ± 0.42	−22.57 ± 0.29	−0.67 ± 0.13	21.84 ± 0.40
7.19	−3.63 ± 0.68	−24.10 ± 0.26	−23.63 ± 0.29	−0.66 ± 0.10	20.70 ± 0.19

of 1.0194 (Kakihana et al., 1977) and the recently measured experimental α_B value of 1.0272 (Klochko et al., 2006). The coral $\delta^{11}B$ values plot above both curves (Fig. 4), although the shape and offset are closest to the seawater $\delta^{11}B$–pH curve calculated using the Kakihana et al. α_B with an average offset of +0.6‰ (±0.3‰ 1SD) for *Porites* sp. and +0.3‰ (±0.3‰ 1SD) for *S. pistillata*.

4. DISCUSSION

4.1. Acclimatization to high pCO_2

Stylophora pistillata and massive *Porites* sp. fragments were exposed to pCO_2 levels of up to sevenfold higher than those predicted to prevail by the end of this century. Following 14 months incubation under reduced pH conditions (8.09, 7.49, and 7.19), all coral fragments survived and added new skeletal calcium carbonate, despite Ω_{arag} values as low as 1.25 and 0.65 (Table 1). These findings suggest that scleractinian coral species will be able to acclimate to a high pCO_2 ocean even if changes in seawater acidity are faster and more dramatic than predicted. Although skeletal growth (Fig. 2) and zooxanthellae density (Fig. 1B and C) were negatively impacted, coral tissue biomass increased in both high pCO_2 treatments (Fig. 1A), and zooxanthellae chlorophyll concentrations increased under the highest pCO_2 conditions (Fig. 1D).

Calcification was negatively affected under increased pCO_2, as recognized in previous short-term coral culture studies (Langdon and Atkinson, 2005; Schneider and Erez, 2006; Anthony et al., 2008). The 55% decrease in skeletal growth of *Porites* sp. (Fig. 2A) are in reasonable agreement with the 40% decrease previously reported (Langdon and Atkinson, 2005; Anthony et al., 2008) for high pCO_2 conditions. The fast-growing branching coral, *S. pistillata*, showed a similar decrease in growth inferred from skeletal surface area. However, smaller changes were measured in buoyant weight (Fig. 2B), implying changes in skeletal morphology toward lower surface-to-volume ratio under reduced pH conditions.

Despite the reduction in skeletal growth, tissue biomass (measured by protein concentration) was found to be higher in both species after 14 months of growth under increased pCO_2 (Fig. 1A). This result is in contrast to Reynaud et al. (2003) who found no change in protein concentration in *S. pistillata* between low, normal and high pCO_2. Fine and Tchernov (2007), however, reported a dramatic increase (orders of magnitude larger than the present study) in protein concentration following incubation of scleractinian Mediterranean corals (*Oculina patagonica* and *Madracis pharencis*) under reduced pH. These findings imply tissue thickening in response to exposure to high pCO_2.

A decrease in zooxanthellae cell density with decreasing pH was recorded in both species (Fig. 1B and C). This trend was accompanied by an increase in chlorophyll concentration per cell at the highest pCO_2 level (Fig. 1D). A similar pattern was reported by Anthony et al. (2008) although the *Porites* corals in their study were exposed to extremely intense light levels (700–1200 μmol photons m^{-2} s^{-1}). In contrast, Reynaud et al. (2003) found no change in cell density and chlorophyll concentration in *S. pistillata* under high pCO_2 and under light intensity and temperature similar to those in the present study.

Acclimation time is an important factor when conducting environmental manipulation experiments. In the present study, long acclimation periods before sampling allowed the coral colonies to reach a steady state in terms of their physiological responses to elevated pCO_2. Differences in physiological parameters between treatments in our study are less extreme than previously reported in the short (8 week) study by Anthony et al. (2008). The lack of differences in zooxanthellae cell density and chlorophyll concentration found by Reynaud et al. (2003) for different pH conditions are possibly due to the even shorter span of their experiment (5 weeks).

4.2. Physiological responses to high pCO_2

The inverse response of skeleton deposition and tissue biomass to changing pCO_2 conditions is consistent with the hypothesis that calcification stimulates zooxanthellae photosynthesis by enhancing CO_2 concentration within the coelenteron (McConnaughey and Whelan, 1997). Under higher pCO_2 conditions, calcification by the coral becomes less important as the source of carbon for photosynthesis by its zooxanthellae, as observed in other marine photosynthetic calcifiers (Goericke and Fry, 1994; Erez et al., 1997). In addition, more CO_2 is released per mole of $CaCO_3$ precipitated at higher CO_2 concentrations due to the shift in seawater carbonate equilibria (Frankignoulle and Canon, 1994). Since calcification is an en-

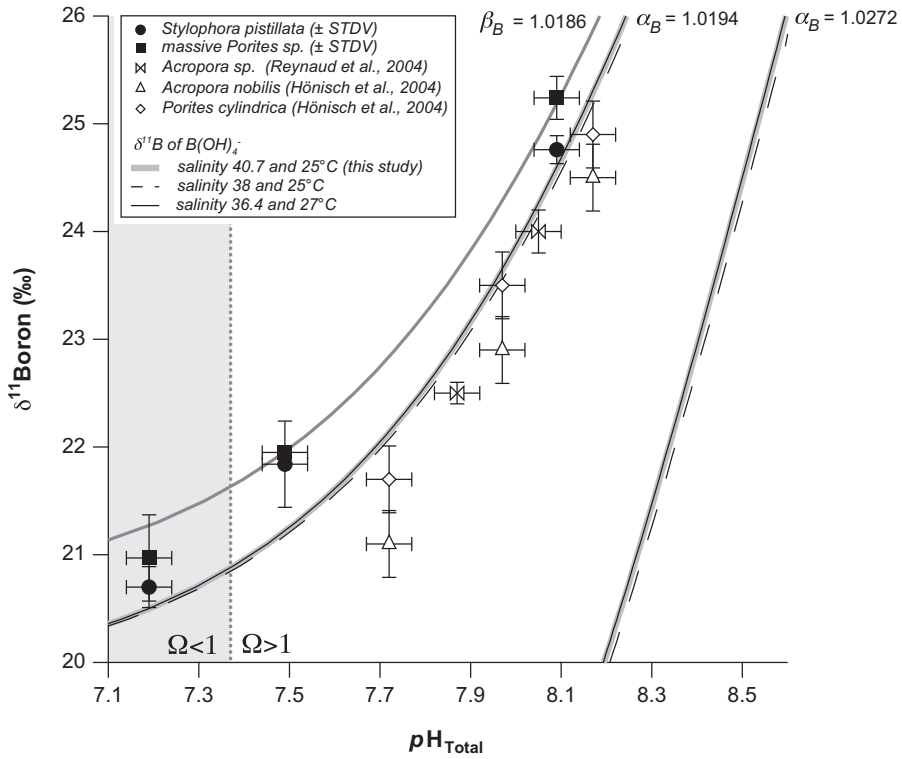

Fig. 4. Boron isotopic composition of *S. pistillata* and massive *Porites* sp. skeletal material cultured at normal (8.09) and reduced pH (7.49 and 7.19) conditions (mean ± SD, $n = 4$ for each treatment). For comparison the data are plotted with previously published δ^{11}B–pH calibration studies from other coral species cultured under elevated pCO_2; *Acropora nobilis* and *Porites cylindrica* (Hönisch et al., 2004) and *Acropora* sp. (Reynaud et al., 2004). The previously published coral data are plotted on the pH_T scale as calculated from measured total alkalinity, DIC and/or pCO_2 for each study. The data is plotted with the derived ($\alpha_B = 1.0194$; Kakihana et al., 1977) and empirical ($\alpha_B = 1.0272$; Klochko et al., 2006) $B(OH)_4^-$ fractionation curves using constants from Zeebe and Wolf-Gladrow (2001) to calculate δ^{11}B–pH. The fractionation curves are calculated assuming a seawater δ^{11}B value of 39.5‰ and taking into account the different experimental conditions for each culture study; 25 °C and a salinity of 40.7 (this study), 25 °C and a salinity of 38 (Reynaud et al., 2004), and 27 °C and a salinity of 36.4 (Hönisch et al., 2004, 2007).

ergy-consuming process requiring the enzyme Ca^{2+}-ATPase to transfer protons across the calicoblastic layer in exchange for Ca^{2+} (Chalker and Taylor, 1975; Tambutté et al., 1996; Al-Horani, 2005), a coral polyp that spends less energy on skeletal growth can instead allocate the energy to tissue biomass (Anthony et al., 2002; Houlbrèque et al., 2004). Similarly, energy-consuming CO_2-concentrating mechanisms (e.g., membrane-bound H^+-ATPase and carbonic anhydrase to convert seawater HCO_3^- into CO_2) become less important for promoting diffusion of CO_2 into cells and increasing photosynthetic efficiency. Hence tissue thickness increases as pH is reduced. Langdon and Atkinson (2005) observed an increase in the photosynthetic activity of zooxanthellate corals under high pCO_2. As a result, a lower population density is required to supply the energy demands of the coral, consistent with our observations (Fig. 1B). Increases in chlorophyll *a* concentrations indicate increased nutrient availability to the zooxanthellae population (Hoegh-Guldberg and Smith, 1989; Rees, 1991). Whether the increase in zooxanthellae chlorophyll concentrations under reduced pH conditions is due to the decrease in zooxanthellae population density and reduced competition for a limited nutrient supply (as also observed during coral bleaching, e.g., Jones, 1997), or due to a shift in availability of species such as NH_4^+ with changing pH (Zeebe and Wolf-Gladrow, 2001), remains to be resolved.

Alternatively, coral may thicken their tissue to increase the buffering layer where pH is biologically regulated in order to create a better separation between the calcification process and the low-Ω_{arag} ambient seawater, which was undersaturated with respect to aragonite in our high-end pCO_2 treatment (Table 1). While reduced calcification rates have traditionally been investigated as a proxy of coral response to environmental stresses (e.g., Barnes and Lough, 1999; Edinger et al., 2000) tissue thickness and protein concentrations are a more sensitive indicator of the health of a colony (Houlbrèque et al., 2004) because energy reserves are preferentially allocated by the coral polyp to calcification (Anthony et al., 2002).

Although higher pCO_2 conditions do not appear to have a strong negative impact on physiological parameters, ocean acidification will have a negative impact on both colony and coral reef ecosystem scales. The reduction in calcification for these coral species will lead to generally weaker skeletons, increasing the risk of physical damage and bioerosion at the colony level (Kleypas et al., 1999b; Carricart-

Ganivet, 2007; Manzello et al., 2008). Ultimately reef ecology will be impacted because the skeletons of both *S. pistillata* and massive *Porites* sp. play key roles in the structure and accretion of the modern reef ecosystem (Kleypas et al., 2001).

4.3. Carbon isotopic response to high pCO_2

Changes in $\Delta^{13}C$ in tissue and zooxanthellae (Fig. 3A and B) agree with previous studies showing that ^{13}C is depleted in marine photosynthetic organisms under elevated pCO_2 (Rau et al., 1992; Laws et al., 1995; Erez et al., 1997). Hence, seasonal variations in tissue and zooxanthellae $\delta^{13}C$ as shown by Swart et al. (2005), reporting enriched values during summer months, may be attributed to variations in oceanic CO_2 concentration associated with primary productivity rates (Bates et al., 1996). The $\Delta^{13}C$ results also support the physiological evidence discussed above that calcification under high pCO_2 conditions becomes less important as the carbon source for zooxanthellate photosynthesis. Because the C isotopic composition of $CO_{2(aq)}$ is lighter by ~8‰ than HCO_3^- at 25 °C (Mook et al., 1974), zooxanthellae $\Delta^{13}C$ values will be reduced under elevated pCO_2 conditions as seawater $CO_{2(aq)}$ replaces HCO_3^-, derived from calcification, as the main source for photosynthesis (Goericke and Fry, 1994; Erez et al., 1997). Zooxanthellate photosynthesis is the primary source of coral nutrition under our experimental conditions and lighter C isotopic compositions in both zooxanthellae and coral tissue are therefore expected. This effect is stronger in *S. pistillata* than *Porites* sp. (Fig. 3A and B) suggesting a greater CO_2 uptake by the zooxanthellae in the faster growing species.

Changes in skeletal $\Delta^{13}C$ are apparently species-specific, with only *Porites* sp. showing a substantial change toward lighter C isotopic compositions at low pH, whereas the *S. pistillata* skeletal C isotopic composition does not change significantly. This suggests that species-specific differences in metabolic fractionation have a dominant effect, and possibly reflects the much higher metabolic rates observed in slow calcifying massive coral compared with fast-growing branched species (Gates and Edmunds, 1999).

Previous studies (Pelejero et al., 2005; Wei et al., 2009) explain a change toward lighter skeletal C isotopic composition under increasing pCO_2 conditions as a direct result of a reservoir effect; i.e., lighter C isotopic composition of DIC due to the isotopically lighter CO_2 emitted by anthropogenic activity. However, our results are corrected for such a reservoir and demonstrate that other, presumably metabolic or other biological factors are in play. Based on our results, the estimated 0.1 pH unit lowering of seawater pH since the mid-19th century would introduce an additional $\delta^{13}C$ shift toward present in a *Porites* sp. $\delta^{13}C$ record of around −0.4‰.

4.4. Skeletal O isotopic response to high pCO_2

The most frequently used coral climate-proxy is $\delta^{18}O$. Coral skeletal $\delta^{18}O$ values are used to trace the $\delta^{18}O$ composition of the ambient seawater and water temperature. Previous studies invoked to relate variations in O isotopic compositions with kinetic disequilibrium. These disequilibrium models all correlate light skeletal O isotopic compositions with fast skeletal growth (Land et al., 1975; Erez, 1978; Weil et al., 1981; McConnaughey, 1989a,b; Allison et al., 1996). Corals generally have slower calcification rates under reduced pH conditions (Fig. 2) (Schneider and Erez, 2006; Anthony et al., 2008; Marubini et al., 2008) and the corresponding heavier skeletal O isotopic compositions (Fig. 3D) would therefore be attributed to lower degrees of disequilibrium. However, the observed strong similarity of the relative $\delta^{18}O$ between the two coral species, in spite of a difference in relative growth-rate reduction with increasing pCO_2, suggest that the cause of the heavier skeletal O isotopic compositions might have to be sought elsewhere. Because HCO_3^- is isotopically heavier than CO_3^{2-}, an alternative explanation for heavier skeletal O isotopic compositions in the low-pH experiments for both species might be a reduction in $[CO_3^{2-}]$. This explanation is favored by Zeebe (1999) to explain the pH effect observed in cultured foraminiferal $\delta^{18}O$ values (Spero et al., 1997).

Whatever the cause, pH-induced changes in $\delta^{18}O$ are significant and must be considered when this isotopic tracer is used as a proxy for past environmental changes, for example sea-surface temperature. Massive *Porites* are the most frequently used coral species used as a paleo-environmental archive, in part because of its regular annual growth bands, which offer a well-defined chronology, and its long life span. *Porites* sp. $\delta^{18}O$ was 0.5‰ and 0.7‰ heavier at pH_T 7.49 and 7.19, respectively, than at pH_T 8.09. This is a large effect considering that a typical calibration of skeletal $\delta^{18}O$ vs. sea-surface temperature for *Porites* is on the order of −0.2‰/1 °C (Gagan et al., 1994). Based on our results a 0.1 pH unit decrease in average oceanic pH since the start of the industrial period (Orr et al., 2005) would introduce an additional −0.08‰ shift in a coral $\delta^{18}O$ record over this time period (equivalent to +0.4 °C).

4.5. $\delta^{11}B$ and pH at the site of calcification

It is evident from this study that both *S. pistillata* and massive *Porites* sp. significantly modify pH at site of calcification relative to the external seawater. Aragonite should not precipitate in the undersaturated conditions of the lowest pH treatment ($pH_T = 7.19$, $\Omega_{arag} = 0.65$; Fig. 4). The deposition of coral skeleton under these conditions demonstrates that both coral species are raising the average pH of the internal calcifying fluid, either driven by shifts in the carbonate system or by active transport of protons, and thereby controlling the aragonite saturation state.

The $\delta^{11}B$ values for both *S. pistillata* and massive *Porites* sp. plot above seawater $\delta^{11}B$–pH borate fractionation curves calculated using either the theoretically derived and commonly applied α_B value of 1.0194 (Kakihana et al., 1977) or the recently measured experimental α_B value of 1.0272 (Klochko et al., 2006). The offset can only be reconciled with the ambient seawater pH values by invoking a process that somehow enriches the skeleton in the heavier isotope or a process that shifts the pH at the site of calcification toward more alkaline conditions. Estimates of the

magnitude of the pH offset depend on the choice of fractionation factor between $B(OH)_3$ and $B(OH)_4^-$.

At face value, the coral $\delta^{11}B$ correspond closest to the shape and values of the seawater $\delta^{11}B$–pH curve of Kakihana et al. (1977) (Fig. 4). Applying the value for α_B of 1.0194, the difference between the seawater $\delta^{11}B$ and coral $\delta^{11}B$ value is equivalent to a shift in pH from ambient seawater to the site of calcification of +0.07, +0.19, and +0.22 pH units for *Porites* sp. at pH treatments 8.09, 7.49, and 7.19, respectively (Fig. 4). Similarly, for *S. pistillata* the $\delta^{11}B$–ΔpH offset is +0.02, +0.17 to +0.11 pH units for pH treatments 8.09, 7.49, and 7.19, respectively.

The Kakihana et al. α_B value has been widely applied in previous boron isotope studies, including the coral $\delta^{11}B$–pH calibration studies for the branching, fast calcifying species of *Acropora* sp. (Hönisch et al., 2004; Reynaud et al., 2004) and *Porites cylindrica* (Hönisch et al., 2004). In contrast to our study, these and other marine carbonate $\delta^{11}B$–pH calibration studies, including foraminifera studies (e.g., Sanyal et al., 1996, 2001; Hönisch et al., 2003; Kasemann et al., 2009), all plot below the Kakihana et al. (1977) curve (Fig. 4). This negative offset has been difficult to explain (Pagani et al., 2005; Hönisch et al., 2007) and the validity of using the Kakihana et al. estimate of α_B to calculate the pH dependent speciation of B has come under scrutiny (Oi, 2000; Liu and Tossell, 2005; Pagani et al., 2005; Sanchez-Valle et al., 2005; Zeebe, 2005; Hönisch et al., 2007). Recently, Rustad and Bylaska (2007) identified a significant error in the Kakihana et al. (1977) vibrational spectrum term for $B(OH)_4^-$ which caused the α_B estimate to be incorrectly low. Our study provides further evidence against the use of the Kakihana et al. (1977) α_B estimate. It is evident at the lowest pH treatment (7.19) that, if α_B was 1.0194, no aragonite with a $\delta^{11}B$ value of 20.88‰ or less should precipitate because conditions would be undersaturated ($\Omega_{arag} = 1$ at $pH_{Total} = 7.37$; Fig. 4). Instead, half of the individual coral samples grown in the 7.19 pH treatment had $\delta^{11}B$ values <20.88‰. The value for α_B must be greater than 1.0200 in order to coincide with conditions where the saturation state is above $\Omega_{arag} = 1$.

The α_B value of 1.0272 ± 0.006 measured by Klochko et al. (2006) produces a much steeper curve (Fig. 4). As a result the $\delta^{11}B$–ΔpH offset from the Klochko et al. (2006) curve increases significantly with decreasing seawater pH and is equivalent to 0.46, 0.85 to 1.08 pH units for *Porites* sp. at treatment pH conditions of 8.09, 7.49, and 7.19 respectively (Fig. 4). The *S. pistillata* $\delta^{11}B$ values are offset by 0.43, 0.84, and 1.06 pH units at pH_T 8.09, 7.49, and 7.19 respectively (Fig. 4). These pH estimates, and the magnitude of the internal pH modification within the coral's tissue, are within the range predicted from physiological processes occurring within symbiont-bearing coral and measured by microsensors (Kühl et al., 1995; Al-Horani et al., 2003a,b). In daylight conditions, microsensor pH measurements give values that are significantly more alkaline within the coral polyp than ambient seawater pH (up to +1 pH units in the calicoblastic layer; Al-Horani et al., 2003a). pH is controlled by the polyp via two ion-transport enzymes; carbonic anhydrase and Ca-ATPase (Al-Horani et al., 2003a,b). Carbonic anhydrase catalyzes the hydration of CO_2, thereby ensuring an abundant supply of HCO_3^- for calcification (Furla et al., 2000). Ca-ATPase transports Ca^{2+} to the site of calcification in exchange for protons, which drives the equilibrium toward $CaCO_3$ formation by converting HCO_3^- to CO_3^{2-} and thereby increasing the aragonite saturation state (McConnaughey and Whelan, 1997). By lowering pCO_2 at the site of calcification, proton removal also initiates a net CO_2 diffusion, further increasing CO_3^{2-} concentrations and the supersaturation of aragonite (Cohen and McConnaughey, 2003).

In addition to physiological control of pH within the coral, the magnitude of the $\delta^{11}B$–pH offset could also be attributed to a shift in the ratio of skeletal material laid down during dark and light calcification. Extreme pH variations have been measured within coral polyps over the daily light/dark cycle (7.3–8.5; Kühl et al., 1995) (7.6–8.5 at the polyp surface and 8.1–9.3 under the calicobastic layer; Al-Horani et al., 2003b), with the highest pHs corresponding to periods of maximum CO_2 consumption by the zooxanthellae; and lower pH values in the dark (Kühl et al., 1995; Al-Horani et al., 2003a,b). Assuming a ratio of dark:light calcification of 1:4 (Furla et al., 2000), the average pH of the calcifying environment could shift by +0.4 pH units relative to the seawater of pH 8.09, for example, if the daytime calcifying pH averages 8.7 and night-time 7.6. Under lower pH conditions, dark calcification is strongly reduced and can even become negative (i.e., skeleton dissolution; Schneider and Erez, 2006), thus the bulk $\delta^{11}B$ represents light calcification that occurs when pH within coral tissue is significantly higher than the environmental pH. Accordingly, offsets between the experimentally-derived curve and the skeletal $\delta^{11}B$ increase with decreasing pH (Fig. 4).

Where species modify and/or control their calcifying environment a specific calibration is essential in the application of the $\delta^{11}B$–pH proxy (Hönisch et al., 2007). Between coral species it is apparent that fast calcifying, branched species typically have lower $\delta^{11}B$ for a given external pH than slower calcifying, massive forms (this study; Hönisch et al., 2004). This study is the first empirical $\delta^{11}B$–pH calibration of massive *Porites* sp.; the most widely used coral for paleo-climate research including paleo-pH reconstruction (e.g., Pelejero et al., 2005; Liu et al., 2009). The external seawater pH can be reconstructed from the internal coral $\delta^{11}B$–pH response by applying the pH–$\delta^{11}B$ equation (Eq. (2)) and substituting a constant (β_B), that best fits the species-specific relationship, for α_B:

$$pH = pK_B^* - \log\left[-\frac{\delta^{11}B_{sw} - \delta^{11}B_{coral}}{\delta^{11}B_{sw} - \beta_B * \delta^{11}B_{coral} - (\beta_B - 1) * 10^3}\right] \quad (3)$$

The best fit value for '$\beta_{B(porites)}$', for the massive *Porites* sp. in this calibration study, is 1.0186 (Fig. 4). It is important to note that the constant $\beta_{B(porites)}$' is not an estimate of the isotopic fractionation factor between $B(OH)_4^-$ and

$B(OH)_3$; a value of 1.0186 for α_B would obviously be incorrect for physio-chemical reasons (e.g., aragonite deposition at $\Omega_{arag} < 1$; Fig. 4). Instead, the α_B value is a means to account for the influence of species-specific vital effects on the incorporation of boron isotopes in marine carbonates.

5. CONCLUSIONS

The long acclimation time of this study allowed the coral colonies to reach a steady state in terms of their physiological responses to elevated pCO_2. As a result, the physiological response to higher pCO_2/lower pH conditions was significant, but less extreme than reported in previous experiments. Our findings suggest that scleractinian coral species will be able to acclimate to a high pCO_2 ocean even if changes in seawater pH are faster and more dramatic than predicted. Although skeletal growth and zooxanthellae density were negatively impacted, coral tissue biomass and zooxanthellae chlorophyll concentrations increased under high pCO_2 conditions. Reduced skeletal growth will have negative implications at colony and ecosystem scales due to increased risk of physical damage and bioerosion, and decreased accretion of reef structure.

Interpretation of the skeletal paleo-environmental proxies $\delta^{13}C$ and $\delta^{18}O$ requires consideration of environmental pCO_2 variations. pH derived changes in $\delta^{13}C$ and $\delta^{18}O$ are significant and must be considered. For example, a 0.1 pH unit decrease in average seawater pH since the start of the industrialization would introduce an additional $-0.08‰$ shift in a coral $\delta^{18}O$ record over this time period (equivalent to +0.4 °C).

The correlated responses of $\delta^{13}C$, tissue growth and skeletal growth support the theory that calcification under high pCO_2 conditions becomes less important as the carbon source for zooxanthellae photosynthesis. The $\delta^{13}C$ response to higher pCO_2/reduced pH is stronger in *S. pistillata* than *Porites* sp. suggesting a greater CO_2 uptake by the zooxanthellae in the faster growing species. Species-based differences in metabolic fractionation also have a dominant effect on skeletal $\delta^{13}C$.

Our study provides the first species-specific empirical calibration for *S. pistillata* and massive *Porites* sp. The $\delta^{11}B$ values for both species plot above seawater $\delta^{11}B$–pH borate fractionation curves calculated using either the theoretically derived α_B value of 1.0194 (Kakihana et al., 1977) or the recently measured experimental α_B value of 1.0272 (Klochko et al., 2006). The $\delta^{11}B$–pH offset, and the deposition of skeleton in seawater with $\Omega_{arag} < 1$, demonstrates the ability of both species to calcify by modifying internal pH toward more alkaline conditions. The increasing offset under higher pCO_2 between skeletal $\delta^{11}B$–pH and external seawater pH can be explained by a shift in the ratio of skeletal material laid down during dark and light calcification and/or greater manipulation of internal pH by the coral polyp via ion-transport enzymes.

ACKNOWLEDGMENTS

The authors thank Murielle Dray for technical assistance, Irena Brailovsky for assistance with isotopic analysis at the Weizmann Institute, and Simon Berkowicz and Lena Hazanov for comments on an early version of the manuscript. The authors also thank the staff of the Interuniversity Institute for Marine Sciences in Eilat for the technical support throughout the experiment and the members of the Bristol Isotope Group (BIG), University of Bristol. This work was supported by the UK Natural Environment Research Council in the form of a NERC fellowship to E.J.H. (NE/D010012/1). The manuscript was greatly improved with help from James Rae, the GCA associate editor Jack Middelburg, and reviews by Peter Swart and an anonymous reviewer.

REFERENCES

Al-Horani F. A. (2005) Effects of changing seawater temperature on photosynthesis and calcification in the scleractinian coral *Galaxea fascicularis* measured with O_2, Ca^{2+} and pH microsensors. *Sci. Marina* **69**, 347–354.

Al-Horani F. A., Al-Moghrabi S. M. and de Beer D. (2003a) The mechanism of calcification and its relation to photosynthesis and respiration in the skeleractinian coral *Galaxea fascicularis*. *Mar. Biol.* **142**, 419–426.

Al-Horani F. A., Al-Moghrabi S. M. and de Beer D. (2003b) Microsensor study of photosynthesis and calcification in the scleractinian coral, *Galaxea fascicularis*: active internal carbon cycle. *J. Exp. Mar. Biol. Ecol.* **288**, 1–15.

Al-Rousan S., Al-Moghrabi S., Patzold J. and Wefer G. (2003) Stable oxygen isotopes in Porites corals monitor weekly temperature variations in the northern Gulf of Aqaba, Red Sea. *Coral Reefs* **22**, 346–356.

Allison N., Tudhope A. W. and Fallick A. E. (1996) Factors influencing the stable carbon and oxygen isotopic composition of *Porites lutea* coral skeletons from Phuket, South Thailand. *Coral Reefs* **15**, 43–57.

Anthony K. R., Connolly S. R. and Willis B. L. (2002) Comparative analysis of energy allocation to tissue and skeletal growth in corals. *Limnol. Oceanogr.* **47**, 1417–1429.

Anthony K. R. N., Kline D. I., Diaz-Pulido G., Dove S. and Hoegh-Guldberg O. (2008) Ocean acidification causes bleaching and productivity loss in coral reef builders. *Proc. Natl. Acad. Sci. USA* **105**, 17442–17446.

Asami R., Yamada T., Iryu Y., Meyer C. P., Quinn T. M. and Paulay G. (2004) Carbon and oxygen isotopic composition of a Guam coral and their relationships to environmental variables in the western Pacific. *Paleogeogr. Paleoclimatol. Paleoecol.* **212**, 1–22.

Barker S., Greaves M. and Elderfield H. (2003) A study of cleaning procedures used for foraminiferal Mg/Ca paleothermometry. *Geochem. Geophys. Geosyst.* **4**, 8407.

Barnes D. J. and Lough J. M. (1999) *Porites* growth characteristics in a changed environment: Misima Island, Papua New Guinea. *Coral Reefs* **18**, 213–218.

Bates N. R., Michaels A. F. and Knap A. H. (1996) Seasonal and interannual variability of the oceanic carbon dioxide system at the U.S. JGOFS Bermuda Atlantic Time-series Site. *Deep-Sea Res. II* **43**, 347–383.

Blamart D., Rollion-Bard C., Meibom A., Cuif J. P., Juillet-Leclerc A. and Dauphin Y. (2007) Correlation of boron isotopic composition with ultrastructure in the deep-sea coral *Lophelia pertusa*: implications for biomineralization and paleo-pH. *Geochem. Geophys. Geosyst.* **8**, Q12001.

Boiseau M. and Juillet-Leclerc A. (1997) H_2O_2 treatment of recent coral aragonite: oxygen and carbon isotopic implications. *Chem. Geol.* **143**, 171–180.

Caldeira K. and Wickett M. E. (2005) Ocean model predictions of chemistry changes from carbon dioxide emissions to the atmosphere and ocean. *J. Geophys. Res. Oceans* **110**, C09S04.

Canadell J. G., Le Quere C., Raupach M. R., Field C. B., Buitenhuis E. T., Ciais P., Conway T. J., Gillett N. P., Houghton R. A. and Marland G. (2007) Contributions to accelerating atmospheric CO_2 growth from economic activity, carbon intensity, and efficiency of natural sinks. *Proc. Natl. Acad. Sci. USA* **104**, 18866–18870.

Carricart-Ganivet J. P. (2007) Annual density banding in massive coral skeletons: result of growth strategies to inhabit reefs with high microborers' activity? *Mar. Biol.* **153**, 1–5.

Chalker B. E. and Taylor D. L. (1975) Light-enhanced calcification and the role of oxidative phosphorylation in calcification of the coral *Acropora cervicornis*. *Proc. R. Soc. Lond. Ser. B* **190**, 323–331.

Cohen A. L. and McConnaughey T. (2003) Geochemical perspectives on coral mineralization. In *Biomineralization* (eds. P. M. Dove, J. J. DeYoreo and S. Weiner). Mineralogical Society of America Geochemical Society, Washington, DC.

Cole J. E., Dunbar R. B., McClanahan T. R. and Muthiga N. A. (2000) Tropical Pacific forcing of decadal SST variability in the Western Indian Ocean over the past two centuries. *Science* **287**, 617–619.

Davies P. S. (1989) Short-term growth measurements of corals using an accurate buoyant weighing technique. *Mar. Biol.* **101**, 389–395.

Dickson A. G. (1990) Standard potential of the reaction: $AgCl(s) + 1/2H_2(g) = Ag(s) + HCl(aq)$, and the standard acidity constant of the ion HSO_4^- in synthetic seawater from 273.15 to 318.15 K. *J. Chem. Thermodyn.* **22**, 113–127.

Dickson A. G. and Millero F. J. (1987) A comparison of the equilibrium constants for the dissociation of carbonic acid in seawater media. *Deep-Sea Res.* **34**, 1733–1743.

Edinger E. N., Limmon G. V., Jompa J., Widjatmoko W., Heikoop J. M. and Risk M. J. (2000) Normal coral growth rates on dying reefs: are coral growth rates good indicators of reef health? *Mar. Pollut. Bull.* **40**, 404–425.

Epstein S. and Mayeda T. (1953) Variation of $\delta^{18}O$ content of waters from natural sources. *Geochim. Cosmochim. Acta* **4**, 213–224.

Erez J. (1978) Vital effect on stable-isotope composition seen in foraminifera and coral skeletons. *Nature* **273**, 199–202.

Erez J., Bouevitch A. and Kaplan A. (1997) *Carbon Isotope Fractionation by Photosynthetic Aquatic Microorganisms: Experiments with Synechococcus PCC7942, and a Simple Carbon Flux Model*. Natl. Res. Council Canada, Vancouver, Canada.

Fine M. and Tchernov D. (2007) Scleractinian coral species survive and recover from decalcification. *Science* **315**, 1811.

Foster G. L. (2008) Seawater pH, pCO_2 and $[CO_3^{2-}]$ variations in the Caribbean Sea over the last 130 kyr: A boron isotope and B/Ca study of planktic foraminifera. *Earth Planet. Sci. Lett.* **271**, 254–266.

Frankignoulle M. and Canon C. (1994) Marine calcification as a source of carbon dioxide – positive feedback of increasing atmospheric CO_2. *Limnol. Oceanogr.* **39**, 458–462.

Furla P., Galgani I., Durand I. and Allemand D. (2000) Sources and mechanisms of inorganic carbon transport for coral calcification and photosynthesis. *J. Exp. Biol.* **203**, 3445–3457.

Gagan M. K., Ayliffe L. K., Beck J. W., Cole J. E., Druffel E. R. M., Dunbar R. B. and Schrag D. P. (2000) New views of tropical paleoclimates from corals. *Quat. Sci. Rev.* **19**, 45–64.

Gagan M. K., Chivas A. R. and Isdale P. J. (1994) High-resolution isotopic records from corals using ocean temperature and mass-spawning chronometers. *Earth Planet. Sci. Lett.* **121**, 539–558.

Gates R. D. and Edmunds P. J. (1999) The physiological mechanisms of acclimatization in tropical reef corals. *Am. Zool.* **39**, 30–43.

Gattuso J. P., Frankignoulle M., Bourge I., Romaine S. and Buddemeier R. W. (1998) Effect of calcium carbonate saturation of seawater on coral calcification. *Global Planet. Change* **18**, 37–46.

Gattuso J. P., Allemand D. and Frankignoulle M. (1999) Photosynthesis and calcification at cellular, organismal and community levels in coral reefs: a review on interactions and control by carbonate chemistry. *Am. Zool.* **39**, 160–183.

Goericke R. and Fry B. (1994) Variations of marine plankton $\delta^{13}C$ with latitude, temperature, and dissolved CO_2 in the world ocean. *Global Biogeochem. Cycles* **8**, 85–90.

Grottoli A. G. (1999) Variability of stable isotopes and maximum linear extension in reef-coral skeletons at Kaneohe Bay, Hawaii. *Mar. Biol.* **135**, 437–449.

Grottoli A. G. (2002) Effect of light and brine shrimp on skeletal $\delta^{13}C$ in the Hawaiian coral *Porites compressa:* a tank experiment. *Geochim. Cosmochim. Acta* **66**, 1955–1967.

Grottoli A. G. and Wellington G. M. (1999) Effect of light and zooplankton on skeletal $\delta^{13}C$ values in the eastern Pacific corals *Pavona clavus* and *Pavona gigantea*. *Coral Reefs* **18**, 29–41.

Heikoop J. M., Dunn J. J., Risk M. J., Sandeman I. M., Schwarcz H. P. and Waltho N. (1998) Relationship between light and the $\delta^{15}N$ of coral tissue: examples from Jamaica and Zanzibar. *Limnol. Oceanogr.* **43**, 909–920.

Heikoop J. M., Dunn J. J., Risk M. J., Schwarcz H. P., McConnaughey T. A. and Sandeman I. M. (2000) Separation of kinetic and metabolic isotope effects in carbon-13 records preserved in reef coral skeletons. *Geochim. Cosmochim. Acta* **64**, 975–987.

Hemming N. G., Guilderson T. P. and Fairbanks R. G. (1998) Seasonal variations in the boron isotopic composition of coral: a productivity signal? *Global Biogeochem. Cycles* **12**, 581–586.

Hemming N. G. and Hanson G. N. (1992) Boron isotopic composition and concentration in modern marine carbonates. *Geochim. Cosmochim. Acta* **56**, 537–543.

Hendy E. J., Gagan M. K., Alibert C. A., McCulloch M. T., Lough J. M. and Isdale P. J. (2002) Abrupt decrease in tropical Pacific sea surface salinity at end of Little Ice Age. *Science* **295**, 1511–1514.

Hoegh-Guldberg O. and Smith G. J. (1989) Influence of the population density of zooxanthellae and supply of ammonium on the biomass and metabolic characteristics of the reef corals *Seriatopora hystrix* and *Stylophora pistillata*. *Mar. Ecol. Prog. Ser.* **57**, 173–186.

Hönisch B., Bijma J., Russell A. D., Spero H. J., Palmer M. R., Zeebe R. E. and Eisenhauer A. (2003) The influence of symbiont photosynthesis on the boron isotopic composition of foraminifera shells. *Mar. Micropaleontol.* **49**, 87–96.

Hönisch B., Hemming N. G., Grottoli A. G., Amat A., Hanson G. N. and Bijma J. (2004) Assessing scleractinian corals as recorders for paleo-pH: empirical calibration and vital effects. *Geochim. Cosmochim. Acta* **68**, 3675–3685.

Hönisch B., Hemming N. G. and Loose B. (2007) Comment on "A critical evaluation of the boron isotope-pH proxy: the accuracy of ancient ocean pH estimates" by M. Pagani D. Lemarchand A. Spivack and J. Gaillardet. *Geochim. Cosmochim. Acta* **71**, 1636–1641.

Houlbrèque F., Tambutté E., Allemand D. and Ferrier-Pagès C. (2004) Interactions between zooplankton feeding, photosynthesis and skeletal growth in the scleractinian coral *Stylophora pistillata*. *J. Exp. Biol.* **207**, 1461–1469.

Jeffrey S. W. and Humphrey G. F. (1975) New spectrophotometric equations for determining Chlorophylls A, B, C1 and C2 in higher plants, algae and natural phytoplankton. *Biochem. Physiol. Pflanzen* **167**, 191–194.

Jones R. J. (1997) Changes in zooxanthellae densities and chlorophyll concentrations in coral during and after a bleaching event. *Mar. Ecol. Prog. Ser.* **158**, 51–59.

Kakihana H., Kotaka M., Satoh S., Nomura M. and Okamoto M. (1977) Fundamental studies on the ion-exchange separation of boron isotopes. *Bull. Chem. Soc. Jpn.* **50**, 158–163.

Kasemann S. A., Schmidt D. N., Bijma J. and Foster G. L. (2009) In situ boron isotope analysis in marine carbonates and its application for foraminifera and palaeo-pH. *Chem. Geol.* **260**, 138–147.

Kleypas J. A., Buddemeier R. W., Archer D., Gattuso J. P., Langdon C. and Opdyke B. N. (1999a) Geochemical consequences of increased atmospheric carbon dioxide on coral reefs. *Science* **284**, 118–120.

Kleypas J. A., McManus J. W. and Menez L. A. B. (1999b) Environmental limits to coral reef development: where do we draw the line? *Am. Zool.* **39**, 146–159.

Kleypas J. A., Buddemeier R. W. and Gattuso J. P. (2001) The future of coral reefs in an age of global change. *Int. J. Earth Sci.* **90**, 426–437.

Kleypas J. A., Feely R. A., Fabry V. J., Langdon C., Sabine C. L. and Robbins L. L. (2006) *Impacts of Ocean Acidification on Coral Reefs And Other Marine Calcifiers*. Report of a workshop sponsored by NSF, NOAA, USGS.

Klochko K., Kaufman A. J., Yao W., Byrne R. H. and Tossell J. A. (2006) Experimental measurement of boron isotope fractionation in seawater. *Earth Planet. Sci. Lett.* **248**, 261–270.

Kühl M., Cohen Y., Dalsgaard T., Jørgensen B. B. and Revsbech N. P. (1995) Microenvironment and photosynthesis of zooxanthellae in scleractinian corals studied with microsensors for O_2, pH and light. *Mar. Ecol. Prog. Ser.* **117**, 159–172.

Land L. S., Lang J. C. and Barnes D. J. (1975) Extension rate: a primary control on the isotopic composition of West Indian (Jamaican) scleractinian reef coral skeleton. *Mar. Biol.* **33**, 221–233.

Langdon C. and Atkinson M. J. (2005) Effect of elevated pCO_2 on photosynthesis and calcification of corals and interactions with seasonal change in temperature/irradiance and nutrient enrichment. *J. Geophys. Res. Oceans* **110**, C09S07.

Laws E. A., Popp B. N., Bidigare R. R., Kennicutt M. C. and Macko S. A. (1995) Dependence of phytoplankton carbon isotopic composition on growth rate and $[CO_2]_{(aq)}$ – theoretical considerations and experimental results. *Geochim. Cosmochim. Acta* **59**, 1131–1138.

Leclercq N., Gattuso J. P. and Jaubert J. (2000) CO_2 partial pressure controls the calcification rate of a coral community. *Global Change Biol.* **6**, 329–334.

Lewis E. and Wallace D. W. R. (1998) Oak Ridge National Laboratory, ORNL/CDIAC-105.

Linsley B. K., Kaplan A., Gouriou Y., Salinger J., deMenocal P. B., Wellington G. M. and Howe S. S. (2006) Tracking the extent of the South Pacific Convergence Zone since the early 1600s. *Geochem. Geophys. Geosyst.* **7**, Q05003.

Liu Y., Liu W. G., Peng Z. C., Mao Y. K., Wei G. J., Sun W. D., He J. F., Liu G. J. and Chou C. L. (2009) Instability of seawater pH in the South China Sea during the mid-late Holocene: evidence from boron isotopic composition of corals. *Geochim. Cosmochim. Acta* **73**, 1264–1272.

Liu Y. and Tossell J. A. (2005) Ab initio molecular orbital calculations for boron isotope fractionations on boric acids and borates. *Geochim. Cosmochim. Acta* **69**, 3995–4006.

Luthi D., Le Floch M., Bereiter B., Blunier T., Barnola J. M., Siegenthaler U., Raynaud D., Jouzel J., Fischer H., Kawamura K. and Stocker T. F. (2008) High-resolution carbon dioxide concentration record 650,000–800,000 years before present. *Nature* **453**, 379–382.

Manzello D. P., Kleypas J. A., Budd D. A., Eakin C. M., Glynn P. W. and Langdon C. (2008) Poorly cemented coral reefs of the eastern tropical Pacific: possible insights into reef development in a high-CO_2 world. *Proc. Natl. Acad. Sci. USA* **105**, 10450–10455.

Marubini F., Ferrier-Pages C., Furla P. and Allemand D. (2008) Coral calcification responds to seawater acidification: a working hypothesis towards a physiological mechanism. *Coral Reefs* **27**, 491–499.

McConnaughey T. (1989a) ^{13}C and ^{18}O isotopic disequilibrium in biological carbonates. I: Patterns. *Geochim. Cosmochim. Acta* **53**, 151–162.

McConnaughey T. (1989b) ^{13}C and ^{18}O isotopic disequilibrium in biological carbonates. II: *In vitro* simulation of kinetic isotope effects. *Geochim. Cosmochim. Acta* **53**, 163–171.

McConnaughey T. and Whelan J. F. (1997) Calcification generates protons for nutrient and bicarbonate uptake. *Earth Sci. Rev.* **42**, 95–117.

McConnaughey T. A., Burdett J., Whelan J. F. and Paull C. K. (1997) Carbon isotopes in biological carbonates: respiration and photosynthesis. *Geochim. Cosmochim. Acta* **61**, 611–622.

Mehrbach C., Culberson C. H., Hawley J. E. and Pytkowicz R. M. (1973) Measurement of the apparent dissociation constants of carbonic acid in seawater at atmospheric pressure. *Limnol. Oceanogr.* **18**, 897–907.

Mook W. G., Bommerso J. C. and Staverma W. H. (1974) Carbon isotope fractionation between dissolved bicarbonate and gaseous carbon-dioxide. *Earth Planet. Sci. Lett.* **22**, 169–176.

Muscatine L. (1990) The role of symbiotic algae in carbon and energy flux in reef corals. In *Coral Reefs* (ed. Z. Dubinsky). Elsevier, Amsterdam.

Nelson S. T. (2000) Sample vial influences on the accuracy and precision of carbon and oxygen isotope ratio analysis in continuous flow mass spectrometric applications. *Rapid Commun. Mass Spectrom.* **14**, 293–297.

Oi T. (2000) Calculations of reduced partition function ratios of monomeric and dimeric boric acids and borates by the ab initio molecular orbital theory. *J. Nucl. Sci. Technol.* **37**(2), 166–172.

Omata T., Suzuki A., Sato T., Minoshima K., Nomaru E., Murakami A., Murayama S., Kawahata H. and Maruyama T. (2008) Effect of photosynthetic light dosage on carbon isotope composition in the coral skeleton: long-term culture of *Porites* spp.. *J. Geophys. Res. Biogeosci.* **113**, 15.

Orr J. C., Fabry V. J., Aumont O., Bopp L., Doney S. C., Feely R. A., Gnanadesikan A., Gruber N., Ishida A., Joos F., Key R. M., Lindsay K., Maier-Reimer E., Matear R., Monfray P., Mouchet A., Najjar R. G., Plattner G. K., Rodgers K. B., Sabine C. L., Sarmiento J. L., Schlitzer R., Slater R. D., Totterdell I. J., Weirig M. F., Yamanaka Y. and Yool A. (2005) Anthropogenic ocean acidification over the twenty-first century and its impact on calcifying organisms. *Nature* **437**, 681–686.

Pagani M., Lemarchand D., Spivack A. and Gaillardet J. (2005) A critical evaluation of the boron isotope-pH proxy: the accuracy of ancient ocean pH estimates. *Geochim. Cosmochim. Acta* **69**, 953–961.

Pelejero C., Calvo E., McCulloch M., Marshall J. F., Gagan M. K., Lough J. M. and Opdyke B. N. (2005) Preindustrial to modern interdecadal variability in coral reef pH. *Science* **309**, 2204–2208.

Pearson P. N. and Palmer M. R. (2000) Atmospheric carbon dioxide concentrations over the past 60 million years. *Nature* **406**, 695–699.

Pierrot D., Lewis E. Wallace, D. W. R. (2006) *MS Excel Program Developed for CO_2 System Calculations*. ORNL/CDIAC-105a. Carbon Dioxide Information Analysis Center, Oak Ridge National Laboratory, U.S. Department of Energy, Oak Ridge, Tennessee.

Rau G. H., Takahashi T., Desmarais D. J., Repeta D. J. and Martin J. H. (1992) The relationship between $\delta^{13}C$ of organic matter and $[CO_2]_{(aq)}$ in ocean surface water – data from a JGOFS site in the northeast Atlantic Ocean and a model. *Geochim. Cosmochim. Acta* **56**, 1413–1419.

Rees T. A. V. (1991) Are symbiotic algae nutrient deficient? *Proc. R. Soc. Lond. Ser. B* **243**, 227–233.

Reynaud S., Leclercq N., Romaine-Lioud S., Ferrier-Pages C., Jaubert J. and Gattuso J. P. (2003) Interacting effects of CO_2 partial pressure and temperature on photosynthesis and calcification in a scleractinian coral. *Global Change Biol.* **9**, 1660–1668.

Reynaud S., Hemming N. G., Juillet-leclerc A. and Gattuso J. P. (2004) Effect of pCO_2 and temperature on the boron isotopic composition of the zooxanthellate coral *Acropora* sp. *Coral Reefs* **23**, 539–546.

Risk M. J., Sammarco P. W. and Schwarcz H. P. (1994) Cross-continental shelf trends in $d^{13}C$ in coral on the Great Barrier Reef. *Mar. Ecol. Prog. Ser.* **106**, 121–130.

Rollion-Bard C., Chaussidon M. and France-Lanord C. (2003) pH control on oxygen isotopic composition of symbiotic corals. *Earth Planet. Sci. Lett.* **215**, 275–288.

Rustad J. R. and Bylaska E. J. (2007) Ab initio calculation of isotopic fractionation in $B(OH)_{3\ (aq)}$ and $B(OH)_4^{-}{}_{(aq)}$. *J. Am. Chem. Soc.* **129**, 2222–2223.

Sabine C. L., Feely R. A., Gruber N., Key R. M., Lee K., Bullister J. L., Wanninkhof R., Wong C. S., Wallace D. W. R., Tilbrook B., Millero F. J., Peng T. H., Kozyr A., Ono T. and Rios A. F. (2004) The oceanic sink for anthropogenic CO_2. *Science* **305**, 367–371.

Sanchez-Valle C., Reynard B., Daniel I., Lecuyer C., Martinez I. and Chervin J.-C. (2005) Boron isotopic fractionation between minerals and fluids: new insights from in situ high pressure-high temperature vibrational spectroscopic data. *Geochim. Cosmochim. Acta* **69**, 4301–4313.

Sanyal A., Hemming N. G., Broecker W. S., Lea D. W., Spero H. J. and Hanson G. N. (1996) Oceanic pH control on the boron isotopic composition of foraminifera: evidence from culture experiments. *Paleoceanography* **11**, 513–517.

Sanyal A., Bijma J., Spero H. and Lea D. W. (2001) Empirical relationship between pH and the boron isotopic composition of *Globigerinoides sacculifer*: implications for the boron isotope paleo-pH proxy. *Paleoceanography* **16**, 515–519.

Schneider K. and Erez J. (2006) The effect of carbonate chemistry on calcification and photosynthesis in the hermatypic coral *Acropora eurystoma*. *Limnol. Oceanogr.* **51**, 1284–1293.

Solomon S., Qin D., Manning M., Chen Z., Marquis M., Averyt K. B., Tigora M. Miller H. L. (Eds.) (2007) Climate Change 2007: The Physical Science Basis. Contribution of Working Group I to the Fourth Assessment Report of the Intergovernmental Panel on Climate Change. Cambridge University Press, Cambridge, UK.

Spero H. J., Bijma J., Lea D. W. and Bemis B. E. (1997) Effect of seawater carbonate concentration on foraminiferal carbon and oxygen isotopes. *Nature* **390**, 497–500.

Stimson J. and Kinzie R. A. (1991) The temporal pattern and rate of release of zooxanthellae from the reef coral *Pocillopora-damicornis* (Linnaeus) under nitrogen-enrichment and control conditions. *J. Exp. Mar. Biol. Ecol.* **153**, 63–74.

Swart P. K., Saied A. and Lamb K. (2005) Temporal and spatial variation in the $\delta^{15}N$ and $\delta^{13}C$ of coral tissue and zooxanthellae in *Montastraea faveolata* collected from the Florida reef tract. *Limnol. Oceanogr.* **50**, 1049–1058.

Tambutté E., Allemand D., Mueller E. and Jaubert J. (1996) A compartmental approach to the mechanism of calcification in hermatypic corals. *J. Exp. Biol.* **199**, 1029–1041.

Wei G. J., McCulloch M. T., Mortimer G., Deng W. F. and Xie L. H. (2009) Evidence for ocean acidification in the Great Barrier Reef of Australia. *Geochim. Cosmochim. Acta* **73**, 2332–2346.

Weil S. M., Buddemeier R. W., Smith S. V. and Kroopnick P. M. (1981) The stable isotope composition of coral skeletons: control by environmental variables. *Geochim. Cosmochim. Acta* **45**, 1147–1153.

Zeebe R. E. (1999) An explanation of the effect of seawater carbonate concentration on foraminiferal oxygen isotopes. *Geochim. Cosmochim. Acta* **63**, 2001–2007.

Zeebe R. E. (2005) Stable boron isotope fractionation between dissolved $B(OH)_3$ and $B(OH)_4^{-}$. *Geochim. Cosmochim. Acta* **69**, 2753–2766.

Zeebe R. E. and Wolf-Gladrow D. A. (2001) *CO_2 in Seawater: Equilibrium, Kinetics, Isotopes*. Elsevier Oceanography Series, vol 65. Elsevier, Amsterdam.

Associate editor: Jack J. Middelburg